

Roles of orbital as a nexus between optical and magnetic properties in cubic RMnO_3 ($\text{R} = \text{La}, \text{Pr}, \text{Nd}, \text{Gd}, \text{Tb}$)

M . W . K im¹, S . J . M oon¹, J . H . J ung², Jaejun Yu³, Sachin Parashar¹, P . M unugavel¹, and T . W . Noh¹¹ReCOE & School of Physics, Seoul National University, Seoul 151-747, Korea²Department of Physics, Inha University, Incheon 402-751, Korea³CSMR & School of Physics, Seoul National University, Seoul 151-747, Korea

We investigated the ab-plane absorption spectra of RMnO_3 ($\text{R} = \text{La}, \text{Pr}, \text{Nd}, \text{Gd}, \text{and Tb}$) thin films. As the R-ion size decreases, we observed a drastic suppression of the 2 eV peak, i.e. the inter-site optical transition between spin- and orbital-aligned states across the Mott gap. We found that both lattice distortion and the corresponding orbital mixing of the ordered orbital state should play an important role in the 2 eV peak suppression. We also found that the 2 eV spectral weight is proportional to the A-type antiferromagnetic ordering temperature, which suggests that the magnetic interaction might be sensitively coupled to the orbital mixing.

PACS numbers: 75.70.-i, 77.90.+k, 78.20.-e

LaMnO_3 has been known as a mother compound of the colossal magnetoresistance (CMR) manganites, where charge, spin, lattice, and orbital degrees of freedom interplay with each other to determine their intriguing physical properties [1, 2]. LaMnO_3 has an orthorhombic structure with four 3d-electrons: three t_{2g} and one e_g electrons. Since three t_{2g} electrons form an orbitally closed shell, many physical properties are believed to be determined by its e_g electron. In its ground state, LaMnO_3 is a Mott-insulator [3, 4, 5] with the A-type spin and the C-type orbital orderings, which are schematically drawn in Figs. 1(a) and 1(b), respectively. The antiferromagnetic (AFM) ordering temperature T_N is about 140 K, and the orbital ordering temperature is around 800 K. The occurrence of the spin- and orbital-ordered state has been understood in terms of the cooperative Jahn-Teller (JT) transition [6].

Rare-earth substitutions of the La ion provide an intriguing phase diagram for RMnO_3 ($\text{R} = \text{rare-earth ion}$) [7], as illustrated in Fig. 1(c). As the R-ion size r_R decreases, the crystal structure of RMnO_3 changes from orthorhombic ($\text{R} = \text{La}\{\text{Dy}\}$) to hexagonal ($\text{R} = \text{Ho}\{\text{Lu}\}$). TbMnO_3 and DyMnO_3 are located near the structural phase boundary, and they have attracted lots of attention recently due to their complicated low temperature magnetic states and multiferroic properties [8]. On the other hand, the magnetic properties of the orthorhombic perovskite RMnO_3 ($\text{R} = \text{La}\{\text{Tb}\}$) has a rather simple R-dependence: T_N decreases with decreasing r_R . Structural deformations, such as buckling and distortion of the MnO_6 octahedra, also increase. According to the Goodenough-Kanamori rule [6, 9], the orbital overlap of electrons should be crucial in determining the magnetic interaction. The rule takes into account the overlap in terms of the Mn-O-Mn bond angle. However, the rapid decrease of T_N with the R-ion substitution is rather unexpected, since the change of \angle is less than 10° . In addition to the lattice distortion due to the \angle variation, a neutron scattering measurement showed that the e_g electron state

should have a mixed character of $\beta z^2 - r^2$ and $x^2 - y^2$ orbitals and that the degree of orbital mixing varies systematically with r_R [10]. This orbital mixing could also affect the orbital overlap of electrons. Therefore, RMnO_3 ($\text{R} = \text{La}\{\text{Tb}\}$) is an ideal system to investigate roles of the lattice distortion and the orbital mixing in numerous physical properties.

Optical spectroscopy has been known to be a powerful tool to investigate the orbital degrees of freedom [3, 4, 11, 12]. In this Letter, we report the ab-plane optical responses of epitaxial RMnO_3 ($\text{R} = \text{La}, \text{Pr}, \text{Nd}, \text{Gd}, \text{and Tb}$) films. We find that the spectral weight of the optical transition across the Mott gap, located around 2 eV, decreases rapidly as r_R decreases. This dramatic reduction of the spectral weight cannot be explained in terms of the conventional model based on the structural variations. We demonstrate that the spectral weight change could be explained by taking account of the structural distortion, i.e., the change of \angle , and the orbital mixing. We also find that the measured spectral weight change is proportional to the variation of T_N .

High quality RMnO_3 ($\text{R} = \text{La}, \text{Pr}, \text{Nd}, \text{Gd}, \text{and Tb}$) thin films were grown on double-side-polished $(\text{LaAlO}_3)_{0.3}(\text{SrAl}_{0.5}\text{Ta}_{0.5}\text{O}_3)_{0.7}$ substrates by using the pulsed laser deposition. From x-ray diffraction measurements, it was found that all the films grew epitaxially with their c-axis perpendicular to the film surfaces. Details of the film growth and their characterization were reported elsewhere [13]. Transmission spectra of the films were measured from 0.4 to 4.0 eV by using a grating spectrophotometer. The absorption coefficients were determined by taking the logarithm of the transmittance, subtracting that of the substrate, and dividing by the

film thickness. Since the normal-incident optical geometry was used, the absorption spectra should come from the ab-plane responses of the films. Figure 2(a) shows the absorption spectra (α) of RMnO_3 at room temperature, where all the samples should be in the C-type orbital ordered state [14]. The spectra of LaMnO_3 are

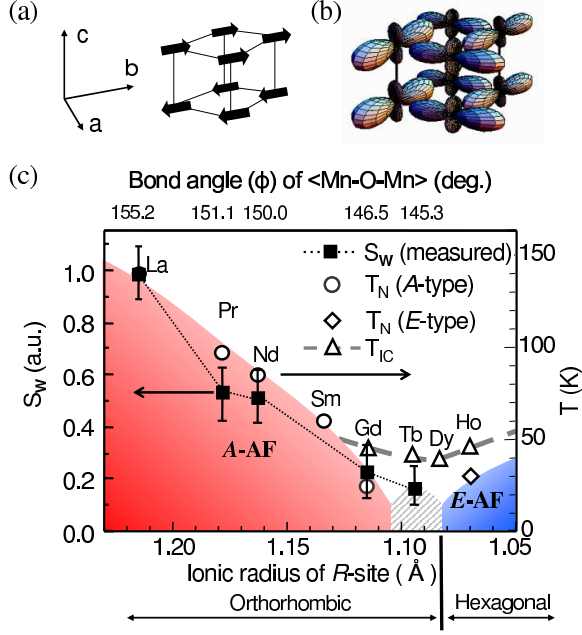


FIG. 1: (color online). (a) The A-type spin and (b) the C-type orbital ordering pattern of electrons at the Mn-sites in LaMnO_3 . (c) A schematic magnetic phase diagram of RMnO_3 , redrawn from Ref. [7]. The spectral weight of 2 eV peak, S_w (the solid square), shows similar R-ion size dependence with the A-type AFM ordering temperature (T) (the open circles). The E-type AFM ordering T (the open diamonds) and the incommensurate spin ordering T (the open triangles) are also shown. The hatched area represents the region where the commensurate spin order and ferroelectric properties emerge.

composed of a peak near 2 eV and much stronger absorption peaks above 3 eV. The higher energy absorption features come from the charge transfer transition from O 2p to Mn 3d [3, 15]. After long debates, numerous recent experiments clearly demonstrated that the 2 eV peak should be interpreted as an inter-site transition across the Mott gap in the orbitally degenerate Hubbard model (ODHM) [3, 4, 5]. As shown in Figs. 1(a) and 1(b), the correlation-induced transition within the ab-plane should occur between the e_g electron states at the neighboring sites in the ferromagnetic-spin (FM) and antiferro-orbital (AFO) configuration [3, 4, 16]. The absorption spectra of other RMnO_3 have very similar spectral features. As r_R decreases, $\langle \phi \rangle$ for the charge transfer transition above 3 eV is nearly independent of the R-ion, however, $\langle \phi \rangle$ for the correlation-induced 2 eV peak

becomes strongly suppressed. To obtain more quantitative information, we estimated the spectral weight S_w by subtracting the charge transfer transition background and integrating $\langle \phi \rangle$ from 0.2 to 2.7 eV. The experimentally determined S_w , marked as the solid squares in Fig. 2(b), becomes drastically suppressed with decreasing r_R .

Such a dramatic decrease of S_w is rather unexpected. All the RMnO_3 compounds, studied in this work, have the same orthorhombic crystal structure and the same spin/orbital ordering pattern, but only with a relatively small variation of $\langle \phi \rangle$. Let us look into the possible role of the structural variations of RMnO_3 in the large S_w change. According to the chemical grip estimate [17], the inter-site transition between the d states can vary approximately as $\cos^4 \phi$. As shown in Fig. 2(b), the contribution of the structural variations to the S_w change could be as large as 30%, but is still much smaller than the experimentally observed S_w changes. Therefore, the electronic structure change due to the structural variation alone cannot explain the large suppression of S_w . To elucidate the origin of the 2 eV peak spectral change, we applied the Fermi golden rule and evaluate the corresponding matrix element. Within the electric dipole approximation [18], S_w becomes proportional to $|\langle f | \hat{p} | i \rangle|^2$. This matrix element can be approximated by the second order perturbation, similarly to the superexchange process, through the oxygen p orbitals:

$$S_w \propto |\langle f | \hat{p} | i \rangle|^2 = \left| \sum_j \langle f | \hat{p} | j \rangle \langle j | i \rangle \right|^2; \quad (1)$$

by assuming that the energy gap remains almost unchanged [19]. Here $|i\rangle$ and $|f\rangle$ represent the wavefunctions of the initial occupied and the final unoccupied Mn e_g orbitals, respectively, of the transition considered. $|j\rangle$ ($= x; y; z$) represents the oxygen p orbitals which bridge the Mn e_g orbitals. For the 2 eV peak, the matrix element can be estimated by the inter-site transition from the occupied e_g state at one site to the unoccupied e_g state at the neighboring site with the FM/AFO configuration, as shown in the inset of Fig. 2(a).

First, let us consider the contribution of the Mn-O-Mn bond angle change in the matrix element. As shown in Fig. 3(a), the buckling of the MnO_6 octahedra in the GdFeO_3 type lattice will cause a decrease in $\langle \phi \rangle$. Without the buckling (i.e. $\langle \phi \rangle = 180^\circ$), the larger lobe of the $3x_1^2 - r_1^2$ -type orbital of a Mn^{3+} site is aligned to face the smaller lobe of the neighboring orbital orthogonally, as shown in Fig. 1(b). As the buckling is turned on, the orbital lobe of an electron at one site will rotate with respect to that at the neighboring site, which will result in a reduction in the inter-site hopping amplitude and thereby a decrease in S_w . To evaluate the changes in $|i\rangle$ and $|f\rangle$ quantitatively, the rotation of the orbitals in the ab-plane was formulated in terms of the rotational transformation of the local (x_2, y_2) coordinates by ϕ with respect to the local (x_1, y_1) coordinates, as shown in Fig.

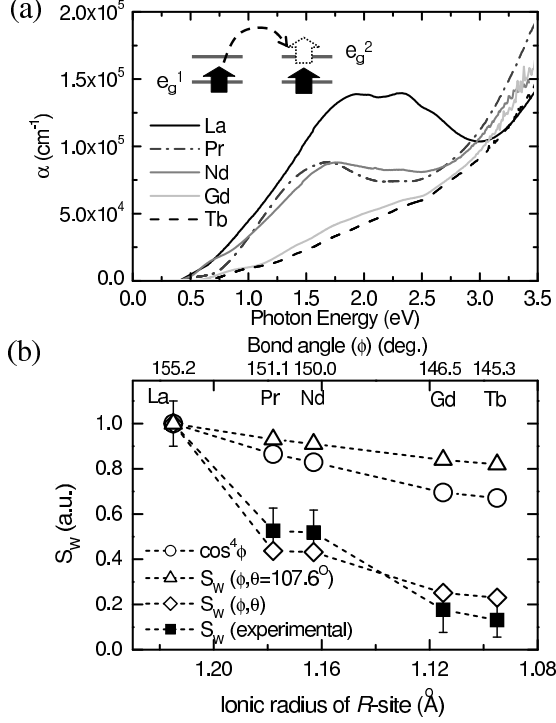


FIG. 2: (a) Absorption spectra of RMnO_3 ($R = \text{La, Pr, Nd, Gd, and Tb}$) thin films at room T. The inset schematically represents the inter-site transition corresponding to the 2 eV peak. (b) The experimental S_W (the solid squares) is compared with the calculation results: the simple estimation of bandwidth change (\cos^4) (the open circles), our model calculation for various ϕ by using the orbitals of LaMnO_3 , i.e., at a fixed θ ($= 107.6^\circ$) (the open triangles), and our model calculation for various ϕ and θ (the open diamonds).

3(a). Here, the local z_1 and z_2 axis directions are assumed to be the same. When the orbital wavefunctions of LaMnO_3 were used, it was found that the orbital rotation effect on S_W is proportional to $\cos^2(\phi)$. As shown in Fig. 1(c), the R-ion substitution in RMnO_3 makes vary from 155.2 to 145.3 [10, 20]. In Fig. 2(b), the calculated values of S_W are plotted with the open triangles. It is obvious that the variation in ϕ alone cannot account for the large change in the experimental S_W .

Now, let us include the orbital mixing contribution. In a cubic MnO_6 octahedron, two e_g orbitals remain doubly degenerate. Under the JT-type distortion along the z -direction, the e_g orbitals become split into two orthogonal orbitals, i.e. $\beta z^2 - r^2$ and $x^2 - y^2$. However, a neutron scattering experiment showed that the actual occupied e_g orbital of RMnO_3 should be a mixed state of these two orbitals depending on the local distortion of the MnO_6 octahedron, and further that the degree of the

orbital mixing will vary depending on r_R [10]. To include the orbital mixing effects in Eq. (1), we constructed realistic Mn e_g orbitals using the orbital mixing angle θ : the occupied orbital at site 1 and the unoccupied orbital at the neighboring site 2 are written as

$$\begin{aligned} |j_1^{\text{occ}}\rangle &= \cos\frac{\theta}{2} \beta z_1^2 - r_1^2 + \sin\frac{\theta}{2} x_1^2 - y_1^2 \\ |j_2^{\text{unocc}}\rangle &= \sin\frac{\theta}{2} \beta z_2^2 - r_2^2 + \cos\frac{\theta}{2} x_2^2 - y_2^2; \end{aligned} \quad (2)$$

where the subscripts in the wavefunctions represent the different local coordinates. The unoccupied orbital, corresponding to the final state of the transition, is orthogonal to the occupied orbital at site 2. To visualize the orbital mixing effects, the occupied orbitals for three different θ values are plotted in Fig. 3(b). Note that the orbital configuration shown in Fig. 1(b) corresponds to $\theta = 180^\circ$, $\phi = 108^\circ$. From Eqs. (1) and (2), we obtained,

$$S_W = f \left(\sin^2 \frac{\theta}{2} \right) \cos^2(\phi) g^2; \quad (3)$$

Using the reported (θ, ϕ) values from the neutron scattering experiment [10, 20], we can estimate the values of $S_W(\theta, \phi)$ and plot them with the open diamonds in Fig. 2(b). The estimated $S_W(\theta, \phi)$ values agree quite well with the measured S_W change, indicating the importance of the orbital mixing. The θ - and ϕ -dependence of S_W is displayed in Fig. 3(c). Note that $\theta = 107.6^\circ$ for LaMnO_3 and $\theta = 114.3^\circ$ for TbMnO_3 . Although the variation of the ϕ value is about 6.7° , smaller than that of the θ value (i.e. about 9.9°), the variation of S_W due to the change in the orbital mixing is larger than that due to the ϕ change. A possible reason is the strong anisotropy in the shape of the orbitals. When $\theta = 90^\circ$, the occupied and unoccupied orbitals given in Eq. (3) have the mean state of the two orthogonal orbitals. As θ increases, the $x^2 - y^2$ orbital enhances the wavefunction overlap and the $\beta z^2 - r^2$ orbital reduces it within the ab -plane, so the mixing of those two orbitals results in the minimum around $\theta = 120^\circ$ in Eq. (3). As shown in Fig. 3(c), RMnO_3 are located near the (θ, ϕ) space where S_W will change rapidly and depend strongly on θ . Thus, the orbital mixing becomes a crucial factor in numerous physical properties of RMnO_3 , including the change in S_W .

The S_W values for various manganites are marked with the solid squares in Fig. 1(c). It is remarkable to note that the R-dependence of the S_W change is quite similar to that for T_N , i.e., the A-type AFM ordering temperature. With decreasing R-ion radius (r_R) from La to Tb, T_N systematically decreases, i.e. from 140 K for LaMnO_3 to nearly zero for TbMnO_3 . Similarly, S_W also becomes significantly reduced for TbMnO_3 as compared with the value for LaMnO_3 . These similar R-dependences of S_W and T_N are rather surprising, since

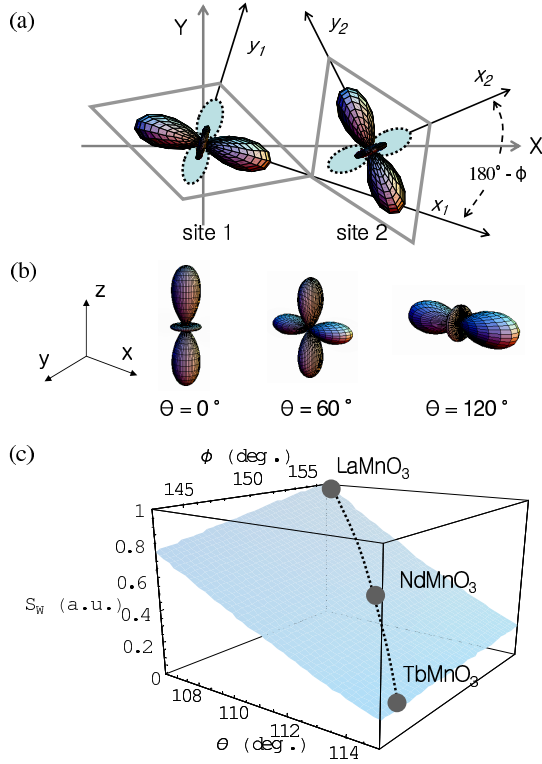


FIG. 3: (color online). The setup is schematically shown for the calculation of the orbital mixing angle (θ) and the Mn-O-Mn bond angle (ϕ) dependent S_W . (a) The local coordinates (x, y) for the MnO₆ octahedra and the Mn e_g orbitals (The orbital lobes drawn with the dashed lines represent the unoccupied orbitals.) (b) The occupied orbitals of selected values. (c) The calculated S_W as a function of θ and ϕ .

the S_W change comes from the ab-plane response while the AFM ordering at T_N occurs along the c-axis.

One possible explanation for this intriguing phenomenon could be an occurrence of additional FM component in the inter-plane interactions due to the buckling of the MnO₆ octahedra. In the undistorted case (i.e., $\phi = 180^\circ$), the A-type spin order should occur due to the FM e_g - e_g interaction within the ab-plane and the AFM t_{2g} - t_{2g} superexchange interaction along the c-axis. Here T_N is mainly determined by the latter, since it is much weaker than the ab-plane FM interaction [21]. When the buckling of the MnO₆ octahedra occurs, however, the overlap of the e_g -orbitals between the Mn-planes brings out a new FM interaction along the c-axis. Although T_N of RMnO₃ should be determined by the competition between the AFM and the FM interactions, the T_N dependence of T_N could be realized mostly by the latter: the AFM interaction should not be so sensitive to the structural change due to the nature of the orbitally

closed t_{2g} levels, but the FM interaction should critically depend on the buckling. Since the FM interaction does appear from the tilting of the MnO₆ octahedra, it could be closely related to S_W , which will be proportional to the square of the electron hopping matrix in the ab-plane. This scenario suggests that the AFM and FM interactions will compete with each other and achieve a balance around TbMnO₃. To explain the anomalous magnetic ground states near the phase boundary, shown in Fig. 1 (c), Kimura et al. recently used a two-dimensional anisotropic neighbor interaction model [22]. Our picture based on a new FM interaction along the c-axis might provide an alternative starting point to explain the intriguing magnetic states near the multiferroic phases.

The conventional Goodenough-Kanamori rule takes into account of the orbital overlap in terms of [6, 9]. Then, the sign of the effective magnetic interactions (i.e. AFM and FM ground states) is expected to change near $\phi = 135^\circ$. In RMnO₃, the GdFeO₃ type distortion can induce the competition between AFM and FM along the c-axis, so one could envisage a disappearance of AFM near 135° . However, as displayed in Fig. 1 (c), the A-type AFM order in the orthorhombic RMnO₃ disappears at $\phi = 145^\circ$. This deviation from the Goodenough-Kanamori rule should originate from the additional contribution of the orbital mixing to the orbital overlap.

In summary, we reported that the spectral weight of the 2 eV peak changes drastically with rare-earth ion size in RMnO₃ ($R = \text{La, Pr, Nd, Gd, and Tb}$). The spectral weight change was successfully understood in terms of the optical matrix element in which Jahn-Teller distortion and the rotation of the orbital were taken into account within the orbitally degenerate Hubbard picture. Similar behaviors between the 2 eV spectral weight and the A-type antiferromagnetic ordering temperature suggest that the superexchange interaction in RMnO₃ might be tuned by the orbital degree of freedom.

We acknowledge valuable discussions with J. S. Lee, K. W. Kim, S. S. A. Seo, K. H. Ahn, P. Littlewood, and P. Horsh. This work was supported by the KOSEF-CRI program and CSCMR SRC, and also supported by the Korean Ministry of Education BK21 project.

corresponding author: twnoh@physa.snu.ac.kr

- [1] Y. Tokura and N. Nagaosa, Science 288, 462 (2000).
- [2] K. Tobe et al, Phys. Rev. B 64, 184421 (2001).
- [3] M. W. Kim et al, New. J. Phys. 6, 156 (2004).
- [4] N. N. Kovaleva et al, Phys. Rev. Lett. 93, 147204 (2004).
- [5] T. Inami et al, Phys. Rev. B 67, 045108 (2003).
- [6] J. B. Goodenough, Phys. Rev. 100, 564 (1955).
- [7] T. Kimura et al, Phys. Rev. B 68, 060404(R) (2003).
- [8] T. Kimura et al, Nature (London) 426, 55 (2003).
- [9] J. Kanamori, J. Phys. Chem. Solids 10, 87 (1959).
- [10] J. A. Alonso et al, Inorg. Chem. 39, 917 (2000).

- [11] M .W .K im et al, Phys.Rev.Lett. 89, 016403 (2002).
- [12] J.S.Lee, M .W .K im , and T.W .Noh, to be published.
- [13] P.M unugave et al, Appl.Phys.Lett. 82, 1908 (2003).
- [14] The orbital ordering temperature increases as the R-ion size decreases. For more information, see Ref. [7].
- [15] J.H .Jung et al, Phys.Rev.B 55, 15489 (1997).
- [16] Its energy cost can be estimated as $U - 3J_H$, where U is the effective on-site Coulomb repulsion energy and J_H is the Hund's rule coupling energy. See Ref. [3, 4].
- [17] W .A .Harrison, in Electronic structure and the properties of solids, (W .H .Freeman and Company, San Francisco, 1980).
- [18] L.C.Lew Yan Voon and L.R.Ram-Mohan, Phys.Rev.B 47, 15500 (1993).
- [19] P.W .Anderson, in Magnetism I, edited by G.T.Rado and H.Suhl (Academic Press, New York, 1963).
- [20] The values for $GdMnO_3$ were obtained by interpolation.
- [21] K.Hirota et al, J.Phys.Soc.Jpn. 65, 3736 (1996).
- [22] This model mimics the frustration, however it does not consider the additional FM interaction along the c-axis.